Published in final edited form as:

Mol Cell. 2016 April 21; 62(2): 222–236. doi:10.1016/j.molcel.2016.03.010.

PRDM16 suppresses MLL leukemia via intrinsic histone methyltransferase activity

Bo Zhou[1], **Jingya Wang**[1], **Shirley Y. Lee**[1], **Jie Xiong**[1], **Natarajan Bhanu**[4], **Qi Guo**[4], **Peilin Ma**[1,5], **Yuqing Sun**[1], **Rajesh C. Rao**[1,3], **Benjamin A. Garcia**, **Jay L. Hess**[1,5], and **Yali Dou**[1,2,*]

[1]Department of Pathology, University of Michigan, Ann Arbor, MI 48109

[2]Department of Biological Chemistry, University of Michigan, Ann Arbor, MI 48109

[3]Ophthalmology & Visual Sciences, University of Michigan, Ann Arbor, MI 48109

[4]Department of Biochemistry and Biophysics, Smilow Center for Translational Research, Perelman School of Medicine, University of Pennsylvania, Philadelphia, PA 19104-5157

SUMMARY

PRDM16 is a transcription cofactor that plays critical roles in development of brown adipose tissue (BAT) as well as maintenance of adult hematopoietic and neural stem cells. Here we report that PRDM16 is a histone H3 K4 methyltransferase on chromatin. Mutation in the N-terminal PR-domain of PRDM16 completely abolishes the intrinsic enzymatic activity of PRDM16. We show that the methyltransferase activity of PRDM16 is required for specific suppression of MLL leukemogenesis both *in vitro* and *in vivo*. Mechanistic studies show that PRDM16 directly activates the SNAG family transcription factor GFI1b, which in turn down regulates the *HOXA* gene cluster. Knockdown GFI1b represses PRDM16-mediated tumor suppression while GFI1b overexpression mimics PRDM16 overexpression. In further support of the tumor suppressor function of PRDM16, silencing PRDM16 by DNA methylation is concomitant with MLL-AF9 induced leukemic transformation. Taken together, our study reveals a previously uncharacterized function of PRDM16 that depends on its PR-domain activity.

[*]**Correspondence:** yalid@umich.edu, Tel: (734) 615-1315, Fax: (734) 763-6476.
[5]Current address: Indiana University, 340 West 10th Street, Fairbanks 6200, Indianapolis, IN 46202-3082

AUTHOR CONTRIBUTION

B.Z designed, performed all experiments and prepared the manuscript. J.W performed RNA-seq analyses. P.M. helped with murine leukemia models. J.X. and Y.S helped with RNA-seq data presentation. S.L helped with the thermo shift assay. N.B, Q.G and B.A.G performed the mass spec experiments, J.L.H provided supervision for J.W and P.M. R.R helped with manuscript writing. Y.D helped with the experimental design and wrote the manuscript.

Accession Number

RNA-seq data sets are deposited with accession number GSE64218.

INTRODUCTION

PRDM16 (also known as MEL, PFM13) encodes a protein of 1,247 amino acids and is comprised of an N-terminal PR domain (PRD1-BF1 and RIZ1 homologous) and several zinc fingers at C-terminus (Figure 1A) (Fog et al., 2012). PRDM16 was initially characterized as an essential factor that regulates the cell-fate switch between brown adipose tissue (BAT) and skeletal myoblasts (Kajimura et al., 2010; Seale et al., 2011). Recent studies show that PRDM16 is highly enriched in multiple adult stem cell lineages and plays important roles in regulating stem cell homeostasis (Aguilo et al., 2011; Chuikov et al., 2010). PRDM16 is also able to suppress stem cell deficiency induced by Bmi1 deletion (Chuikov et al., 2010). Loss-of-function of PRDM16 leads to multi-lineage defects including hematopoiesis, neurogenesis and palotogenesis *in vivo* (Bjork et al., 2010; Deneault et al., 2009; Endo et al., 2012; Horn et al., 2011).

PRDM16 resides in chromosome 1p36, which is frequently deleted or rearranged in multiple human cancers (Martinez-Climent et al., 2003; Mochizuki et al., 2000; Morishita, 2007; White et al., 2005). At least two protein isoforms are encoded by *PRDM16:* the full-length PRDM16 and the shorter isoform PRDM16S (also known as MELS) that lacks the PR domain (Nishikata et al., 2003). These two PRDM16 isoforms are transcribed from distinct transcription start sites (TSS) and are subject to differential regulation by DNA methylation (Yoshida et al., 2004). In particular, TSS of *PRDM16*, but not *PRDM16S*, resides in large regions of CpG islands (CGIs). *PRDM16* silencing by DNA hypermethylation has been described in several cancers (Morishita, 2007; Tan et al., 2014). Consistent with differential regulation in cancer, aberrant expression of *PRDM16S* has been described in leukemia (Du et al., 2005b; Mochizuki et al., 2000; Nishikata et al., 2003; Xiao et al., 2006). Since genetic loss of function study in mouse models often simultaneously disrupts both PRDM16 isoforms, the specific function of PRDM16, especially its PR-domain, in cancer remains unclear.

PRDM16 is a transcription co-activator that acts in concert with transcription factors such as PPAR-γ (peroxisome proliferator-activated receptor), PPAR-β, PGC-1α as well as CEBP-β (CCAAT/enhancer-binding protein) in promoting expression of thermogenic genes *in vivo* (Kajimura et al., 2009; Seale et al., 2008; Seale et al., 2007). PRDM16 also directly interacts with the MED1 subunit of the Mediator complex and enhances thyroid hormone receptor (TR)-driven transcription in a Mediator-dependent manner (Iida et al., 2015). These functions involve direct interactions between PRDM16 C-terminal zinc fingers and transcription cofactors. It remains unclear whether the N-terminal PR-domain plays a role in transcription regulation. The PR domain of PRDM16 is a variant of the SET (Suv39, E(z) and Trithorax) domain that is commonly found in histone lysine methyltransferases (HKMT) (Jenuwein and Allis, 2001). It was reported that the PR domain of PRDM16 has intrinsic HKMT activity and is able to mono-methylate a 6-mer H3 peptide that harbors histone H3 lysine (K) 9 (H3K9) *in vitro* (Pinheiro et al., 2012). However, it was not determined whether PRDM16 is able to methylate other lysine residues on histones and whether it has substrate specificity on nucleosomes (Pinheiro et al., 2012). Furthermore, the function of the intrinsic methyltransferase activity of PRDM16 was not directly established in cells (Pinheiro et al., 2012).

By rigorous biochemical analyses, we demonstrate that PRDM16 is a highly specific histone methyltransferase that target histone H3 lysine 4 (H3K4) on nucleosomes. Mutating H3K4 to glutamine (Q) completely abolishes PRDM16 dependent histone methylation *in vitro*. Furthermore, the HKMT activity of PRDM16 is essential for suppressing mixed lineage leukemia (MLL). Overexpression or depletion of PRDM16 significantly alters MLL progression *in vivo*. Mechanistic studies reveal an important regulatory network involving *PRDM16*, the SNAG family transcription factor *GFI1b* and *HOXA* genes that is regulated by PRDM16 activity. Taken together, our studies provide insights into the sequence of events that lead to MLL by uncovering a PR-domain dependent tumor suppression function for PRDM16.

RESULTS

PRDM16 is a specific H3 K4 methyltransferase on chromatin

In order to establish the substrate specificity of PRDM16 on chromatin, we purified the PR/SET domains of PRDM16 and a PRDM16 mutant (PRDM16mut) carrying two amino acid mutations (C113F and V115G) using the insect cell expression system (Figure 1A and 1B). The PR-domain mutations did not affect thermostability of PRDM16 (Supplemental Figure 1A), suggesting minimal perturbation of the protein structure. The methyltransferase activity of PRDM16 was first tested on free histones. PRDM16 specifically methylates histone H3 but not other core histones (Figure 1C). To explore the substrate specificity, we generated histone mutants, in which lysine at positions 4, 9, 27, 36, or 79 was each mutated to glutamine (Q). We found that wild-type PRDM16 failed to methylate H3K4Q while it was able to methylate H3 that contained other lysine mutation (i.e. K9Q, K27Q, K36Q and K79Q) *in vitro* (Figure 1D). As the control, PRDM16mut showed no HKMT activity under the same condition, confirming that H3K4 methylation was due to the intrinsic activity of the PR-domain (Figure 1D). To examine PRDM16 specificity on nucleosomes, we used the reconstituted nucleosomes that contained wild type H3, H3K4Q, H3K9Q or H3K27Q mutant as the substrate. As shown in Figure 1E, PRDM16 could not methylate H3K4Q-containing nucleosomes whereas it had robust activity on nucleosomes comprised of H3K9Q or H3K27Q. Both mass spectrometry (Supplemental Figure 1B) and immunoblot (Supplemental Figure 1C) showed that PRDM16 was able to mono- and di-methylate H3K4 in nucleosomes. No tri-methylation of H3K4 or methylation of other lysine residues of H3 was detected by mass spec (Supplemental Figure 1B and data not shown). Taken together, we conclude that the PR domain of PRDM16 has intrinsic HKMT activity that is specific for nucleosomal H3 K4 *in vitro*.

PRDM16 methyltransferase activity is essential to suppress MLL-AF9 leukemogenesis

Since PRDM16 is a direct target of mixed lineage leukemia protein (MLL1, also called MLL, ALL1, HTRX and KMT2A) (Artinger et al., 2013), we wondered whether PRDM16 and more specifically, its PR domain, played a role in *MLL*-rearranged leukemia. We co-transduced Lin^- murine bone marrow (BM) cells with retroviruses expressing *Prdm16*, inactive *Prdm16mut* or the PR-less *Prdm16S* isoform together with *MLL-AF9* (Supplemental Figure 1D). The proliferations of co-transduced *MLL-AF9+Prdm16, MLL-AF9+Prdm16mut* or *MLL-AF9+Prdm16S* cells were measured by the liquid proliferation

and myeloid colony formation assays (Figure 2A). As shown in Figure 2B and 2C, overexpression of *Prdm16* completely inhibited *MLL-AF9*-induced leukemic transformation. It reduced cell proliferation and clonogenicity of *MLL-AF9* cells. No compact colonies on the methylcellulose medium were observed for *MLL-AF9+Prdm16* cells beyond second plating (Figure 2C and 2D). Furthermore, Wright-Giemsa staining showed that *MLL-AF9+Prdm16* co-transduced cells largely differentiated into monocyte-like cells. (Figure 2C, bottom panel). In contrast, *MLL-AF9*, *MLL-AF9+Prdm16mut* and *MLL-AF9+Prdm16S* cells formed compact colonies in serial plating and the transformed cells remained undifferentiated by Wright-Giemsa staining (Figure 2C and 2D). To confirm that endogenous *Prdm16* inhibits MLL-AF9 leukemogenesis, we co-transduced *MLL-AF9* with either control shRNA or *Prdm16* shRNA (Supplemental Figure 1E). We found that *Prdm16* knockdown significantly enhanced clonogenicity of the *MLL-AF9*-transformed cells in serial plating (Two-way ANOVA analysis, $p<0.0001$, Figure 2D) and increased cell proliferation in liquid culture (Figure 2B). These results indicate that PRDM16 suppresses *MLL-AF9*-mediated leukemic transformation *in vitro*.

PRDM16 specifically inhibits the MLL leukemic transformation

To determine whether PRDM16 suppresses leukemic transformation by other oncogenes, we performed similar studies in which primary BM cells were transformed by additional *MLL* fusion genes (i.e. *MLL-AF6* and *MLL-ENL*) as well as non-*MLL* oncogene *E2A-HLF*. Interestingly, we found that *Prdm16*, but not *Prdm16mut*, specifically inhibits leukemic transformation by MLL fusion genes. It reduced myeloid colony formation on methylcellulose and decreased cell proliferation in liquid culture (Figure 2E and 2F and Supplemental Figure 1F). Interestingly, overexpression of *Prdm16*, *Prdm16S* or *Prdm16mut* had indistinguishable effects when co-transduced with *E2A-HLF* (Supplemental Figure 1G). They did not affect cell proliferation in liquid culture (Supplemental Figure 2A), colony formation in serial plating (Supplemental Figure 2B) or maintenance of leukemic blasts (Supplemental Figure 2C). Together, these results suggest that PRDM16 specifically inhibits *MLL* fusion mediated leukemogenesis *in vitro* and this function requires the PR domain activity.

PRDM16 alters MLL leukemia progression *in vivo*

To further explore the role of *PRDM16* and its HMT activity in *MLL* leukemogenesis, we isolated BM cells from C57BL/6 mice ($CD45.2^+$), and co-transduced them with *MLL-AF9+vector control*, *MLL-AF9+Prdm16* or *MLL-AF9+Prdm16mut*, respectively. About $1x10^5$ cells were competitively transplanted into the lethally irradiated B6.SJL mice ($CD45.1^+$), together with supporting $CD45.1^+$ cells (Muntean et al., 2010). The engrafted mice, six in each cohort, were monitored for acute myeloid leukemia (AML). Flow cytometric analyses at 48-hour post-transplantation showed similar number of engrafted $CD45.2^+$ BM cells in recipient mice (Supplemental Figure 2D). Importantly, mice receiving *MLL-AF9+vector control* or *MLL-AF9+Prdm16mut* developed acute myeloid leukemia (AML) about 80 days post transplantation (Figure 3A). They showed obvious emaciation and significant weight loss (Supplemental Figure 2E). All mice receiving *MLL-AF9+vector control* or *MLL-AF9+Prdm16mut* cells died before 110 days with splenomegaly and hepatomegaly (Figure 3B and Supplemental Figure 2E). Leukemic blasts were detected in

peripheral blood and infiltrated into bone, spleen, liver and lung of these mice (Figure 3C and Supplemental Figure 2F). In contrast, none of the *MLL-AF9+Prdm16* recipient mice developed AML by the end point of the study (Figure 3A, Log-rank (Mantel-Cox) test, p<0.0001). No notable defects in peripheral blood and hematopoietic organs in *MLL-AF9+Prdm16* recipient mice were observed (Figure 3B and 3C). Flow cytometric analysis of isolated BM cells and splenocytes from each cohort supported the histologic findings. Significant amplification of $CD45.2^+$ cells was found in BM and spleens of *MLL-AF9* and *MLL-AF9+Prdm16mut* recipient mice. Majority of these cells expressed $Mac1^{high}$ and $Gr\text{-}1^{high}$ surface makers, as expected for AML (Muntean et al., 2010) (Figure 3D and Supplemental Figure 2G). In contrast, very few $CD45.2^+$ cells were found in *MLL-AF9+Prdm16* recipients, consistent with a disease-free phenotype. These results suggest an essential role of PRDM16 HMT activity in suppressing *MLL-AF9* leukemogenesis *in vivo*.

In contrast to *Prdm16* overexpression, depletion of endogenous *Prdm16* during *MLL-AF9* transduction greatly accelerated MLL leukemogenesis. We co-transduced $CD45.2^+$ BM cells with retroviruses expressing MLL-AF9 and *Prdm16* shRNAs or control shRNAs and transplanted the cells into $CD45.1^+$ recipient mice. As shown in Figure 3A, all mice receiving cells expressing *MLL-AF9+Prdm16* shRNA developed AML. Importantly, onset of AML in these mice was ~50 days post transplantation, which was significantly earlier than mice that were grafted with *MLL-AF9*-transduced cells alone. All mice receiving *MLL-AF9+Prdm16* shRNA cells died before 84 days (Figure 3A, Log-rank (Mantel-Cox) test, p=0.0012). Histologic studies showed that these mice had typical AML phenotypes that were indistinguishable from *MLL-AF9* leukemia (Figure 3B–3D and Supplemental Figure 2E–2G). Given the much shortened disease latency for mice grafted with *MLL-AF9+Prdm16shRNA* cells, our results signify that PRDM16 alters the trajectory of MLL leukemogenesis *in vivo* and that down regulation of endogenous PRDM16 is probably one of the rate-limiting steps for the onset of MLL leukemia.

PRDM16 suppresses leukemic transformation by repressing the *HoxA* gene cluster

To better understand the mechanism by which PRDM16 HKMT activity suppresses MLL leukemogenesis, we performed Illumina-based RNA-sequencing (RNA-seq). To identify the PRDM16 activity-dependent transcriptome, we focused on genes that showed differential expression between *MLL-AF9+Prdm16* and *MLL-AF9+Prdm16mut*-transduced cells. A comparison of transcriptomes from these two groups revealed a total of 2,751 genes that showed more than two-fold differential expression (False discovery rate (FDR) <=0.05) (Figure 4A, 4B and Supplemental Table S1). 1,540 genes were down regulated (green) and 1,211 genes were up regulated (red) in *MLL-AF9+Prdm16mut*-transduced cells (Figure 4A and 4B). The global changes in gene expression suggest that PRDM16 HMT activity is important for transcriptome-wide regulation in *MLL-AF9*-transduced cells. Gene ontology (GO) analyses showed that Prdm16 regulates broad biological processes including immune responses, signal transduction, hematopoietic differentiation and metabolic pathways via its methyltransferase activity (Supplemental Figure 3A and Supplemental Table S2). Importantly, gene set enrichment analyses (GSEA) showed significant negative correlations of PRDM16 transcriptome with gene signatures associated with MLL leukemic cells (Bernt et al., 2011; Wang et al., 2005), granulocytes (Chambers et al., 2007) and embryonic stem

cells gene (Ben-Porath et al., 2008) (Figure 4C). These results demonstrate that PRDM16 HMT activity shapes the *Lin*$^-$ BM cell transcriptome during *MLL-AF9* mediated-leukemogenesis.

To determine whether the PRDM16-associated gene expression pattern in *MLL-AF9* mediated-leukemogenesis is distinct from that of non-MLL leukemia, we co-transduced *Lin*$^-$ BM cells with *E2A-HLF+Prdm16* and *E2A-HLF+Prdm16mut* constructs and performed similar RNA-seq experiments. Interestingly, while we found no differences in clonogenicity and proliferation between *E2A-HLF+Prdm16* and *E2A-HLF+Prdm16mut*-transduced cells during E2A-HLF transformation (Supplement Figure 1), we found that PRDM16 inactivation led to transcriptome-wide changes. Specifically, in our comparison of the transcriptomes of *E2A-HLF+Prdm16* and *E2A-HLF+Prdm16mut*-transduced cells, we found at least two-fold difference in 1,412 genes, with 808 genes (red) up regulated and 604 genes (green) down regulated (Figure 4A). A comparison of these genes with those altered in *MLL-AF9* cells co-transduced with *Prdm16* and *Prdm16mut* revealed only a small set of genes (~158) was regulated by the PR-domain activity in both *MLL-AF9* and *E2A-HLF* co-transduced cells (Figure 4B). Among them, 77 genes were down regulated and 82 genes were up regulated upon *PRDM16* inactivation in both cells (Supplemental Table S3). A closer examination of the 82 genes that were commonly up regulated upon *Prdm16* inactivation during *MLL-AF9* and *E2A-HLF*-mediated transformation showed that almost all *HoxA* cluster genes were significantly up regulated (Figure 4D). The RNA-seq results were confirmed by real-time RT-PCR (Supplemental Figure 3B–3D). These results suggest that PRDM16 mediated *Hox A* repression is probably a general regulatory mechanism that is independent of specific oncogene context. Consistent with this notion, PRDM16 mediated repression of *Hox A* genes was also observed in normal BM cells transduced with PRDM16 (Supplemental Figure 3E). PRDM16 inactivation did not affect expression of other *Hox* clusters (e.g. *Hox B*) (Supplemental Figure 3F). We speculate that the specific inhibition of MLL leukemia by PRDM16 is probably due to the reliance of MLL on *Hox A* overexpression (see discussion).

Gfi1b is a key mediator of PRDM16 regulation of Hox A genes

To determine whether PRDM16 directly repressed *HoxA* gene cluster, we performed chromatin immunoprecipitation (ChIP) experiment for the affinity tagged-exogenous PRDM16. We could not find enrichment of PRDM16 at any *HoxA* gene (Figure 4E and data not shown). This result suggests that PRDM16 probably represses *HoxA* genes indirectly. To identify the PRDM16 direct target(s) that mediate *HoxA* repression, we focused on the 77 PRDM16 targets that were down regulated upon co-transduction of *Prdm16mut* in both MLL-AF9 and E2A-HLF cells (Figure 4F and Supplemental Table S3). These down regulated genes included several important hematopoietic transcription factors (e.g. KLF2, ETS1 and GFI1b) implicated in HSPC function. Among them, GFI1b appeared as a potentially appealing candidate target of PRDM16. GFI1b belongs to the GFI subfamily of the SNAG zinc finger containing transcription factors restricted to hematopoietic stem cells (Chiang and Ayyanathan, 2013; Saleque et al., 2007; van der Meer et al., 2010). The homolog of GFI1b, GFI1, has been reported to repress gene expression by recruiting the CoREST complex (Chowdhury et al., 2013; Saleque et al., 2007). We first confirmed

specific up regulation of *GFI1b* upon overexpression of wild type PRDM16 (Figure 5A). ChIP experiments showed that both PRDM16 and PRDM16mut directly bound to the *Gfi1b* promoter, but not the control *Hoxa9 locus*, in MLL-AF9 cells (Figure 5B). Importantly, an increase of H3K4me2 at the *Gfi1b* promoter was detected upon binding of PRDM16, but not PRDM16mut (Figure 5C). Concomitant increase in RNA polymerase II (Pol-II) binding was also observed at the *Gfi1b* promoter upon PRDM16 binding (Figure 5D). These results support a direct role of the PR-domain activity in *Gfi1b* activation.

Since the GFI1b homolog, GFI1, has been reported to repress *Hox A* gene expression by recruiting the CoREST complex (Chowdhury et al., 2013; Saleque et al., 2007), we tested whether GFI1b also binds to *Hox A* loci and recruits the CoREST/LSD1 complex. Indeed, GFI1b bound to three consensus sequences near *Hoxa3, Hoxa7* and *Hoxa9* (Figure 5E). The binding of GFI1b correlated with decrease in H3K4me2 and Pol-II binding at these loci (Supplemental Figure 4A and Figure 5D). Consistent with previous studies (Chowdhury et al., 2013; Saleque et al., 2007), immunoprecipitation using HA-tagged GFI1b showed that GFI1b physically interacted with the CoREST/LSD1 complex (Figure 5F) and GFI1b-depended recruitment of LSD1 and CoREST was observed in *MLL-AF9+Gfi1b* cells (Supplemental Figure 4B and 4C). In corroboration of GFI1b as a key mediator of PRDM16 function, overexpression of PRDM16 also led to recruitment of LSD1 and CoREST to *Hox A* cluster, albeit indirectly (Supplemental Figure 4D and 4E). Importantly, overexpression of -PRDM16 led to increase in the heterochromatin marks such as H3K9me1 and H3K9me2 (Supplemental Figure 4F and 4G). It also led to reduced chromatin binding of MLL-AF9 protein at *Hox A* genes, consistent with reduced chromatin accessibility (Figure 5G). These changes led to repression of all *Hox A* gene expression (Figure 5H).

Gfi1b mimics PRDM16 in suppressing *MLL-AF9* leukemic transformation

To further establish that GFI1b functions downstream of PRDM16 in suppressing MLL leukemia, we knocked down endogenous *Gfi1b* in *MLL-AF9+Prdm16* co-transduced cells by two independent shRNAs (Supplemental Figure 5A). *Gfi1b* depletion in *MLL-AF9+Prdm16* co-transduced cells led to re-activation of *Hox A* genes that were repressed by PRDM16 overexpression (Figure 5I). Consistent with gene expression changes, *Gfi1b* depletion rescued the inhibitory effects of PRDM16 overexpression on *MLL-AF9* leukemic transformation (Figure 6A and 6B) without affecting the PRDM16 protein level (Supplemental Figure 5A, bottom panel). Cell proliferation and clonogenicity of *GFI1b*-depleted *MLL-AF9+Prdm16* cells were similar to those of *MLL-AF9* cells (Figure 6A and 6B). On the contrary, overexpression of *Gfi1b* significantly inhibited leukemogenesis when co-transduced with MLL-AF9 *in vitro* (Supplemental Figure 5B–E). Consistent with *in vitro* studies, transplantation of *MLL-AF9+Gfi1b* co-transduced BM cells into lethally irradiated recipients did not give rise to AML *in vivo* (Figure 6C) despite similar engraftment efficiency as the *MLL-AF9* cells (Supplemental Figure 6A). All mice survived beyond the end point of the study (115 days) (Figure 6C) without detectable hematological abnormalities (Figure 6D–6F and Supplemental Figure 6B–6D).

Silencing endogenous PRDM16 accompanies MLL-AF9 leukemic transformation

Hitherto, we demonstrated that PRDM16 played essential roles in suppressing MLL leukemic transformation via its HKMT activity. These results raised the question of whether silencing endogenous *Prdm16* is a prerequisite for *MLL-AF9*-mediated leukemic transformation, especially given the relatively long latency of MLL leukemia (Ayton and Cleary, 2001; Krivtsov and Armstrong, 2007). Interestingly, we found a gradual reduction of *Prdm16* transcripts following MLL-AF9 transduction; at 35 days, these transcripts were barely detectable (Figure 7A). Concomitantly, a gradual decrease of *Gfi1b* and an increase of *Hoxa9* expression were found in these cells (Figure 7A). Next we examined whether *Prdm16* silencing was due to DNA methylation since the TSS of *Prdm16* resides within a large CpG island (CGI) (Figure 7B). We measured DNA methylation after 7 or 35 days of *MLL-AF9* transduction by bisulfite sequencing. We found that out of 10 tested CpGs, three of them (i.e. 3, 4 and 9) showed dramatic increase of DNA methylation. While these CpGs were methylated at ~30–50% at early stage of transformation, they were fully methylated in completely transformed *MLL-AF9* leukemia cells, consistent with silencing of *Prdm16* in these cells (Figure 7B). Dynamic change in DNA methylation during the course of leukemic transformation was further confirmed by 5-methylcytosine immunoprecipitation (MeDIP) at the *Prdm16* TSS (Figure 7C). Importantly, the regulation of *Prdm16* by DNA methylation was reversible. When we treated the *MLL-AF9*-transduced cells with 50nM DNA methyltransferase (DNMT1) inhibitor decitabine (Nie et al., 2014), a dose-dependent reactivation of endogenous *Prdm16* (Supplemental Figure 7A) and significant decrease of DNA methylation at *Prdm16* CGIs were observed (Supplemental Figure 7B). Consistently, we found that *MLL-AF9* leukemia cells showed increased sensitivity to decitabine (GI_{50} 44.6nM) as compared to *E2A-HLF* leukemia cells (GI_{50} 82.14nM, Supplemental Figure 7C). Decitabine induced both apoptosis and differentiation of the *MLL-AF9* leukemia cells (Supplemental Figure 7D and 7E). Interestingly, knockdown *Prdm16* in the *MLL-AF9* leukemia cells compromised the effects of decitabine (GI_{50} 65.06nM, Supplemental Figure 7C), suggesting that decitabine blocks MLL leukemia, at least in part, by reactivating endogenous *Prdm16*.

DISCUSSION

Here we report that PRDM16 is a highly specific H3 K4 methyltransferase on chromatin and its intrinsic activity is essential for suppressing MLL1-rearranged acute leukemia. The tumor suppression function of PRDM16 is mediated by the SNAG family transcription factor GFI1b, which negatively regulates the *Hox A* gene cluster through recruiting the LSD1/CoREST complex. Overexpression of PRDM16 or GFI1b inhibits initiation of MLL leukemogenesis while knockdown PRDM16 significantly accelerates the disease trajectory of MLL leukemia *in vivo*. We further demonstrate that silencing endogenous PRDM16 by DNA methylation accompanies leukemic transformation induced by MLL-AF9.

The PR domain of PRDM16 is required for tumor suppression in MLL

PRDM16 is one of the 17 PRDM gene family proteins in human. A previous study reported that PRDM16 was an H3K9me1 HKMT, based on an *in vitro* HKMT assay using a 6-mer H3 peptide with H3K9 as the only lysine residue (Pinheiro et al., 2012). Our study here

shows that PRDM16 is a highly specific HKMT for histone H3 K4 methylation. Mutation of H3 K4 completely abolished PRDM16 activity on nucleosomes *in vitro* and PRDM16 binding at the GFI1b promoter leads to increase of H3K4me2, but not H3K9me, in cells (Figure 5). These results argue that PRDM16 is a H3K4 specific methyltransferase on chromatin. We would like to point out that PRDM16 has extremely low activity on short peptides (i.e. 6–20aa) as compared to the nucleosome substrate (data not shown), which we have used for the mass spec and immunoblot studies. We also would like to point out that PRDM16 seems to have more robust mono-methylation activity *in vitro*, although we cannot rule out different detection efficiency of H3K4me1 and H3K4me2 peptides by mass spec due to propionylation of H3K4me1.

Importantly, we show that PRDM16 specifically suppresses MLL leukemogenesis via its PR-domain function. Since the PR domain mutation does not affect the thermostability of PRDM16 (Supplemental Figure 1A) or its interaction with known protein partners (e.g. PGC1 and MED1) (data not shown), it is likely that the intrinsic activity of the PR domain is specifically required for tumor suppression function of PRDM16. Several previous studies have shown that overexpression of PR-less PRDM16S isoform, but not PRDM16, is leukemogenic: 1) leukemogenic translocation in AMLs mostly involves PRDM16S, but not full length PRDM16 (Quentin et al., 2011; Shimizu et al., 2000); 2) PRDM16S is selectively overexpressed in adult T cell leukemia (Yoshida et al., 2004); 3) aberrant expression of PRDM16S by retroviral insertion promotes immortalization of murine bone marrow progenitors and blocks granulocytic differentiation (Du et al., 2005a; Nishikata et al., 2003); 4) overexpression of *Prdm16S* in *p53* null bone marrow cells induces AML with full penetrance (Shing et al., 2007); and 5) overexpression of both *Prdm16S* and *Hoxb4* led to myeloid expansion and leukemia (Yu et al., 2014). These studies suggest that loss of the PR-domain is compatible with leukemogenesis. Interestingly, our studies show that overexpression of *Prdm16S* or *Prdm16mut* in MLL leukemia does not affect cell proliferation (Figure 2), suggesting that loss of PR-domain or its activity is not sufficient to promote leukemic transformation in this context. Future studies on the context-dependent functions of PRDM16 and PRDM16S are necessary to further delineate the role of PRDM16 and PRDM16S in leukemia in future.

PRDM16 depletion shortens the latency of MLL *in vivo*

MLL1 rearranged leukemia has long latency, leading to the hypothesis of a ‘two-hit’ model (Ayton and Cleary, 2001; Krivtsov and Armstrong, 2007). This model implies that in addition to the balanced MLL1 translocation, subsequent genetic or epigenetic alterations are needed for leukemic transformation. However, the evolutionary trajectory that leads from the initial lesion to the eventual development of leukemia is not well understood and epigenetic alterations concurrent with *HOXA9* overexpression are not clear. Our studies here show that PRDM16 plays a critical and specific role in suppressing MLL disease progression. Concurrent knockdown of *PRDM16* during MLL-AF9 transduction significantly shortens disease latency while overexpression of *PRDM16* blocks leukemogenesis (Figure 3). Although we cannot rule out that MLL inhibition by *PRDM16* overexpression is due to increased latency beyond end point of the study, the significant anti-

correlation between *PRDM16* level and onset of MLL is striking. This result is also consistent with down regulation of PRDM16 in MLL patients (Hazourli et al., 2006).

Several recent genomic studies show that genetic and epigenetic heterogeneity within the pre-leukemic HSPC translates into variegated diagnostic and prognostic signatures (Corces-Zimmerman et al., 2014; Shlush et al., 2014). We speculate that epigenetic silencing of PRDM16 in pre-LSCs by local stochastic DNA methylation (Gruber and Wu, 2014) likely renders initial selective advantage for some pre-leukemic stem cells (pre-LSCs) by de-repressing HOXA genes. Unchecked HOXA expression that is essential for MLL maintenance (Chen et al., 2008), in turn, drives successive waves of clonal selection and expansion of LSCs that eventually leads to fully developed leukemia. Consistent with this model, gradual silencing of *PRDM16* and concomitant increase of *HOXA9* are observed upon MLL-AF9 transformation (Figure 7A). Furthermore, enforced expression or depletion of PRDM16 results in significantly altered disease progression, probably by blocking or accelerating these processes respectively. Since the pre-LSC provides a silent reservoir for the formation of LSCs in fully transformed leukemia, future delineation of pre-leukemic genetic and epigenetic events in MLL will facilitate the development of lasting cures for the disease by rationally eradiating all pre-LSC populations.

PRDM16 indirectly regulates HOXA cluster genes

Our study shows that PRDM16 is a master regulator of transcription in the pre-leukemic HSPC. Inactivating PRDM16 methyltransferase activity induces global changes in transcriptome of both MLL-AF9 and E2A-HLF cells. Importantly, PRDM16 regulates multiple pleiotropic transcription factors such as ETS1 (Findlay et al., 2013), KLF2 (Novodvorsky and Chico, 2014) and GFI1b. These results are consistent with previous studies that PRDM16 is required for HSPC homeostasis (Deneault et al., 2009) and overexpression of Prdm16 leads to increased HSC numbers and activity in *vivo* (Chuikov et al., 2010). More importantly, PRDM16 plays an important role in controlling the level of *HOXA* genes in hematopoietic cells. The regulation of *HOXA* genes by PRDM16 is consistent with a previous study that overexpression of PRDM16 could partially rescue Bmi1-deficiency in HSC (Chuikov et al., 2010), which also represses HOXA genes (Bracken et al., 2006). Deregulation of *HOXA* genes such as *HOXA9* by either enforced overexpression or chromosomal rearrangements is sufficient to drive leukemic transformation (Argiropoulos and Humphries, 2007). In fact, elevated *HOXA9* expression is reported in over 50% of AML patients and is also associated with myeloproliferative disorders (Owens and Hawley, 2002). Therefore, maintaining *HOXA9* expression at appropriate level is important for balancing HSPC proliferation and malignant transformation. We show that PRDM16 plays a key role to repress *HOXA* gene expression in HSPC by activating transcription repressor GFI1b, which directly binds to HOXA loci and recruits histone demethylase LSD1 (Chowdhury et al., 2013; Saleque et al., 2007). Since PRDM16 is a direct target of *MLL1* (Artinger et al., 2013), it is possible that PRDM16-dependent *HOXA9* repression completes a feedback regulatory loop that prevents the unchecked up regulation of *HOXA9* by MLL1 in normal HSPC. Given recent progresses in therapeutic targeting factors that up regulates HOXA9 in MLL (Rao and Dou, 2015), it will

be interesting to explore whether reactivating endogenous HOXA9 repressive pathways (e.g. PRDM16) also has therapeutic value in future.

EXPERIMENTAL PROCEDURE

PRDM16 expression and purification

His-tagged PR domains of PRDM16 (9–517aa) were expressed from Sf9 insect cells. The recombinant proteins were purified by Ni-NAT magnetic agarose matrix (QIAGEN).

In vitro HMT assay

Preparation of recombinant histones and nucleosomes and in vitro HMT assay were performed as previously described (Wu et al., 2013). Details see Supplemental Method.

Flow Cytometry analysis

Cells from peripheral blood, BM, or spleen were harvested for immunophenotypic analysis. Analyses were performed on LSRII Files and analyzed by FlowJo (TreeStar) software.

DNA Methylation Analysis

MLL-AF9 stable leukemia cells (~$2X10^6$) were collected for genomic DNA extraction after 72 hours Decitabine treatment (Abcam ab1200842). DNA bisulfite conversion was performed using Methylation-Gold™ Kit (ZYMO RESEARCH D5005). Regions for detection were amplified by PCR and cloned into the TOPO vector (Invitrogen). The sequencing was done by DNA Sequencing Core facility at University of Michigan.

Retroviral Transduction and Myeloid Colony Formation Assay

The retroviral vectors were transduced to the BM cell as previously described (Muntean et al., 2010). Retroviruses were collected after 48 or 72 hours and transduce BM cells by spinoculation with 90 minutes at 3000rpm. After retroviral transduction, cells were selected for 3 days before plating in methylcelllose medium (M3234, STEMCELL Technologies) with 10ng/ml IL-3, 10ng/ml IL-6, 100ng/ml SCF, 10ng/ml GM-CSF. After three rounds of plating, Plates were scanned and the clone numbers were accounted. Cells harvested at the end of the experiment were cytospin and stained with Hema 3 Stain Kit (Thermo Fisher Scientific).

Murine Bone Marrow (BM) Transformation Assays

Six to eight week old C57BL/6 mice were treated with 4 mg/mouse 5-fluorouacil before BM cell isolation. BM cells were isolated using the EasySep® Mouse Hematopoietic Progenitor Cell Enrichment Kit (STEMCELL Technologies). Lin^- BM cells were isolated from 6~8-week-old C57BL/6 mice and transduced with retroviruses. After selection by 1mg/ml G418 or 1.5μg/ml puromycin for 4 days, the cells were counted and injected through the tail vein into cohorts of lethal irradiated (900 rads) B6.SJL mice. Donor and supporting cells (from B6.SJL mice), $1X10^5$ each, were injected into each mouse. Recipient mice were checked daily for leukemia development. Tissues from mice at the end of the study were fixed with 10% formalin, embedded and subject to histology studies (Tan et al., 2011). All animal

experiments in this study were approved by the University of Michigan Committee on Use and Care of Animal and Unit for Laboratory Animal Medicine (ULAM).

CHIP Assay

The CHIP assay was performed as previously described (Dou et al., 2005). Antibody information can be found in Supplemental Information.

RNA-sequencing experiment

The RNA was extracted using Trizol reagent (Ambion) and further purified by RNeasy Mini kit (QIAGEN) following manufacture's protocol. 10ng of total RNAs from each sample were used for preparation of lllumina sequencing library. RNA sequencing was performed on Illumina HiSeq2000 at University of Michigan DNA sequencing core facility. Details for data analyses are shown in Supplemental Information.

Supplementary Material

Refer to Web version on PubMed Central for supplementary material.

Acknowledgments

The work are supported by NIGMS (GM082856), American Cancer Society (ACS) and Leukemia and Lymphoma Society Scholar grants to YD, by NIH R01 CA151425 grant to JLH and by NIGMS (GM110174) and the Leukemia and Lymphoma Society Dr. Robert Arceci Scholar Award to BAG. We are grateful to Drs. Jiandie Lin for the PRDM16 cDNA, Patrick Seale for the anti-PRDM16 antibody and Mark Schlissel for GFI1b cDNA.

REFERENCE

Aguilo F, Avagyan S, Labar A, Sevilla A, Lee DF, Kumar P, Lemischka IR, Zhou BY, Snoeck HW. Prdm16 is a physiologic regulator of hematopoietic stem cells. Blood. 2011; 117:5057–5066. [PubMed: 21343612]

Argiropoulos B, Humphries RK. Hox genes in hematopoiesis and leukemogenesis. Oncogene. 2007; 26:6766–6776. [PubMed: 17934484]

Artinger EL, Mishra BP, Zaffuto KM, Li BE, Chung EK, Moore AW, Chen Y, Cheng C, Ernst P. An MLL-dependent network sustains hematopoiesis. Proc Natl Acad Sci U S A. 2013; 110:12000–12005. [PubMed: 23744037]

Ayton PM, Cleary ML. Molecular mechanisms of leukemogenesis mediated by MLL fusion proteins. Oncogene. 2001; 20:5695–5707. [PubMed: 11607819]

Ben-Porath I, Thomson MW, Carey VJ, Ge R, Bell GW, Regev A, Weinberg RA. An embryonic stem cell-like gene expression signature in poorly differentiated aggressive human tumors. Nat Genet. 2008; 40:499–507. [PubMed: 18443585]

Bernt KM, Zhu N, Sinha AU, Vempati S, Faber J, Krivtsov AV, Feng Z, Punt N, Daigle A, Bullinger L, et al. MLL-rearranged leukemia is dependent on aberrant H3K79 methylation by DOT1L. Cancer Cell. 2011; 20:66–78. [PubMed: 21741597]

Bjork BC, Turbe-Doan A, Prysak M, Herron BJ, Beier DR. Prdm16 is required for normal palatogenesis in mice. Hum Mol Genet. 2010; 19:774–789. [PubMed: 20007998]

Bracken AP, Dietrich N, Pasini D, Hansen KH, Helin K. Genome-wide mapping of Polycomb target genes unravels their roles in cell fate transitions. Genes & development. 2006; 20:1123–1136. [PubMed: 16618801]

Chambers SM, Boles NC, Lin KY, Tierney MP, Bowman TV, Bradfute SB, Chen AJ, Merchant AA, Sirin O, Weksberg DC, et al. Hematopoietic fingerprints: an expression database of stem cells and their progeny. Cell Stem Cell. 2007; 1:578–591. [PubMed: 18371395]

Chen W, Kumar AR, Hudson WA, Li Q, Wu B, Staggs RA, Lund EA, Sam TN, Kersey JH. Malignant transformation initiated by Mll-AF9: gene dosage and critical target cells. Cancer Cell. 2008; 13:432–440. [PubMed: 18455126]

Chiang C, Ayyanathan K. Snail/Gfi-1 (SNAG) family zinc finger proteins in transcription regulation, chromatin dynamics, cell signaling, development, and disease. Cytokine Growth Factor Rev. 2013; 24:123–131. [PubMed: 23102646]

Chowdhury AH, Ramroop JR, Upadhyay G, Sengupta A, Andrzejczyk A, Saleque S. Differential transcriptional regulation of meis1 by Gfi1b and its co-factors LSD1 and CoREST. PloS one. 2013; 8:e53666. [PubMed: 23308270]

Chuikov S, Levi BP, Smith ML, Morrison SJ. Prdm16 promotes stem cell maintenance in multiple tissues, partly by regulating oxidative stress. Nat Cell Biol. 2010; 12:999–1006. [PubMed: 20835244]

Corces-Zimmerman MR, Hong WJ, Weissman IL, Medeiros BC, Majeti R. Preleukemic mutations in human acute myeloid leukemia affect epigenetic regulators and persist in remission. Proc Natl Acad Sci U S A. 2014; 111:2548–2553. [PubMed: 24550281]

Deneault E, Cellot S, Faubert A, Laverdure JP, Frechette M, Chagraoui J, Mayotte N, Sauvageau M, Ting SB, Sauvageau G. A functional screen to identify novel effectors of hematopoietic stem cell activity. Cell. 2009; 137:369–379. [PubMed: 19379700]

Dou Y, Milne TA, Tackett AJ, Smith ER, Fukuda A, Wysocka J, Allis CD, Chait BT, Hess JL, Roeder RG. Physical association and coordinate function of the H3 K4 methyltransferase MLL1 and the H4 K16 acetyltransferase MOF. Cell. 2005; 121:873–885. [PubMed: 15960975]

Du Y, Jenkins NA, Copeland NG. Insertional mutagenesis identifies genes that promote the immortalization of primary bone marrow progenitor cells. Blood. 2005a; 106:3932–3939. [PubMed: 16109773]

Du Y, Spence SE, Jenkins NA, Copeland NG. Cooperating cancer-gene identification through oncogenic-retrovirus-induced insertional mutagenesis. Blood. 2005b; 106:2498–2505. [PubMed: 15961513]

Endo K, Karim MR, Taniguchi H, Krejci A, Kinameri E, Siebert M, Ito K, Bray SJ, Moore AW. Chromatin modification of Notch targets in olfactory receptor neuron diversification. Nat Neurosci. 2012; 15:224–233.

Findlay VJ, LaRue AC, Turner DP, Watson PM, Watson DK. Understanding the role of ETS-mediated gene regulation in complex biological processes. Adv Cancer Res. 2013; 119:1–61. [PubMed: 23870508]

Fog CK, Galli GG, Lund AH. PRDM proteins: important players in differentiation and disease. Bioessays. 2012; 34:50–60. [PubMed: 22028065]

Gruber M, Wu CJ. Evolving understanding of the CLL genome. Semin Hematol. 2014; 51:177–187. [PubMed: 25048782]

Hazourli S, Chagnon P, Sauvageau M, Fetni R, Busque L, Hebert J. Overexpression of PRDM16 in the presence and absence of the RUNX1/PRDM16 fusion gene in myeloid leukemias. Genes Chromosomes Cancer. 2006; 45:1072–1076. [PubMed: 16900497]

Horn KH, Warner DR, Pisano M, Greene RM. PRDM16 expression in the developing mouse embryo. Acta Histochem. 2011; 113:150–155. [PubMed: 19853285]

Iida S, Chen W, Nakadai T, Ohkuma Y, Roeder RG. PRDM16 enhances nuclear receptor-dependent transcription of the brown fat-specific Ucp1 gene through interactions with Mediator subunit MED1. Genes & development. 2015; 29:308–321. [PubMed: 25644605]

Jenuwein T, Allis CD. Translating the histone code. Science. 2001; 293:1074–1080. [PubMed: 11498575]

Kajimura S, Seale P, Kubota K, Lunsford E, Frangioni JV, Gygi SP, Spiegelman BM. Initiation of myoblast to brown fat switch by a PRDM16-C/EBP-beta transcriptional complex. Nature. 2009; 460:1154–1158. [PubMed: 19641492]

Kajimura S, Seale P, Spiegelman BM. Transcriptional control of brown fat development. Cell Metab. 2010; 11:257–262. [PubMed: 20374957]

Krivtsov AV, Armstrong SA. MLL translocations, histone modifications and leukaemia stem-cell development. Nat Rev Cancer. 2007; 7:823–833. [PubMed: 17957188]

Martinez-Climent JA, Alizadeh AA, Segraves R, Blesa D, Rubio-Moscardo F, Albertson DG, Garcia-Conde J, Dyer MJ, Levy R, Pinkel D, et al. Transformation of follicular lymphoma to diffuse large cell lymphoma is associated with a heterogeneous set of DNA copy number and gene expression alterations. Blood. 2003; 101:3109–3117. [PubMed: 12406872]

Mochizuki N, Shimizu S, Nagasawa T, Tanaka H, Taniwaki M, Yokota J, Morishita K. A novel gene, MEL1, mapped to 1p36.3 is highly homologous to the MDS1/EVI1 gene and is transcriptionally activated in t(1;3)(p36;q21)-positive leukemia cells. Blood. 2000; 96:3209–3214. [PubMed: 11050005]

Morishita K. Leukemogenesis of the EVI1/MEL1 gene family. Int J Hematol. 2007; 85:279–286. [PubMed: 17483069]

Muntean AG, Tan J, Sitwala K, Huang Y, Bronstein J, Connelly JA, Basrur V, Elenitoba-Johnson KS, Hess JL. The PAF complex synergizes with MLL fusion proteins at HOX loci to promote leukemogenesis. Cancer Cell. 2010; 17:609–621. [PubMed: 20541477]

Nie J, Liu L, Li X, Han W. Decitabine, a new star in epigenetic therapy: the clinical application and biological mechanism in solid tumors. Cancer Lett. 2014; 354:12–20. [PubMed: 25130173]

Nishikata I, Sasaki H, Iga M, Tateno Y, Imayoshi S, Asou N, Nakamura T, Morishita K. A novel EVI1 gene family, MEL1, lacking a PR domain (MEL1S) is expressed mainly in t(1;3)(p36;q21)-positive AML and blocks G-CSF-induced myeloid differentiation. Blood. 2003; 102:3323–3332. [PubMed: 12816872]

Novodvorsky P, Chico TJ. The role of the transcription factor KLF2 in vascular development and disease. Prog Mol Biol Transl Sci. 2014; 124:155–188. [PubMed: 24751430]

Owens BM, Hawley RG. HOX and non-HOX homeobox genes in leukemic hematopoiesis. Stem Cells. 2002; 20:364–379. [PubMed: 12351808]

Pinheiro I, Margueron R, Shukeir N, Eisold M, Fritzsch C, Richter FM, Mittler G, Genoud C, Goyama S, Kurokawa M, et al. Prdm3 and Prdm16 are H3K9me1 methyltransferases required for mammalian heterochromatin integrity. Cell. 2012; 150:948–960. [PubMed: 22939622]

Quentin S, Cuccuini W, Ceccaldi R, Nibourel O, Pondarre C, Pages MP, Vasquez N, Dubois d'Enghien C, Larghero J, Peffault de Latour R, et al. Myelodysplasia and leukemia of Fanconi anemia are associated with a specific pattern of genomic abnormalities that includes cryptic RUNX1/AML1 lesions. Blood. 2011; 117:e161–e170. [PubMed: 21325596]

Rao RC, Dou Y. Hijacked in cancer: the KMT2 (MLL) family of methyltransferases. Nat Rev Cancer. 2015; 15:334–346. [PubMed: 25998713]

Saleque S, Kim J, Rooke HM, Orkin SH. Epigenetic regulation of hematopoietic differentiation by Gfi-1 and Gfi-1b is mediated by the cofactors CoREST and LSD1. Mol Cell. 2007; 27:562–572. [PubMed: 17707228]

Seale P, Bjork B, Yang W, Kajimura S, Chin S, Kuang S, Scime A, Devarakonda S, Conroe HM, Erdjument-Bromage H, et al. PRDM16 controls a brown fat/skeletal muscle switch. Nature. 2008; 454:961–967. [PubMed: 18719582]

Seale P, Conroe HM, Estall J, Kajimura S, Frontini A, Ishibashi J, Cohen P, Cinti S, Spiegelman BM. Prdm16 determines the thermogenic program of subcutaneous white adipose tissue in mice. J Clin Invest. 2011; 121:96–105. [PubMed: 21123942]

Seale P, Kajimura S, Yang W, Chin S, Rohas LM, Uldry M, Tavernier G, Langin D, Spiegelman BM. Transcriptional control of brown fat determination by PRDM16. Cell Metab. 2007; 6:38–54. [PubMed: 17618855]

Shimizu S, Suzukawa K, Kodera T, Nagasawa T, Abe T, Taniwaki M, Yagasaki F, Tanaka H, Fujisawa S, Johansson B, et al. Identification of breakpoint cluster regions at 1p36.3 and 3q21 in hematologic malignancies with t(1;3)(p36;q21). Genes Chromosomes Cancer. 2000; 27:229–238. [PubMed: 10679911]

Shing DC, Trubia M, Marchesi F, Radaelli E, Belloni E, Tapinassi C, Scanziani E, Mecucci C, Crescenzi B, Lahortiga I, et al. Overexpression of sPRDM16 coupled with loss of p53 induces myeloid leukemias in mice. J Clin Invest. 2007; 117:3696–3707. [PubMed: 18037989]

Shlush LI, Zandi S, Mitchell A, Chen WC, Brandwein JM, Gupta V, Kennedy JA, Schimmer AD, Schuh AC, Yee KW, et al. Identification of pre-leukaemic haematopoietic stem cells in acute leukaemia. Nature. 2014; 506:328–333. [PubMed: 24522528]

Tan J, Jones M, Koseki H, Nakayama M, Muntean AG, Maillard I, Hess JL. CBX8, a polycomb group protein, is essential for MLL-AF9-induced leukemogenesis. Cancer Cell. 2011; 20:563–575. [PubMed: 22094252]

Tan SX, Hu RC, Liu JJ, Tan YL, Liu WE. Methylation of PRDM2, PRDM5 and PRDM16 genes in lung cancer cells. International journal of clinical and experimental pathology. 2014; 7:2305–2311. [PubMed: 24966940]

van der Meer LT, Jansen JH, van der Reijden BA. Gfi1 and Gfi1b: key regulators of hematopoiesis. Leukemia. 2010; 24:1834–1843. [PubMed: 20861919]

Wang J, Iwasaki H, Krivtsov A, Febbo PG, Thorner AR, Ernst P, Anastasiadou E, Kutok JL, Kogan SC, Zinkel SS, et al. Conditional MLL-CBP targets GMP and models therapy-related myeloproliferative disease. Embo J. 2005; 24:368–381. [PubMed: 15635450]

White PS, Thompson PM, Gotoh T, Okawa ER, Igarashi J, Kok M, Winter C, Gregory SG, Hogarty MD, Maris JM, et al. Definition and characterization of a region of 1p36.3 consistently deleted in neuroblastoma. Oncogene. 2005; 24:2684–2694. [PubMed: 15829979]

Wu L, Lee SY, Zhou B, Nguyen UT, Muir TW, Tan S, Dou Y. ASH2L regulates ubiquitylation signaling to MLL: trans-regulation of H3 K4 methylation in higher eukaryotes. Mol Cell. 2013; 49:1108–1120. [PubMed: 23453805]

Xiao Z, Zhang M, Liu X, Zhang Y, Yang L, Hao Y. MEL1S, not MEL1, is overexpressed in myelodysplastic syndromes patients with t(1;3)(p36;q21). Leuk Res. 2006; 30:332–334. [PubMed: 16102824]

Yoshida M, Nosaka K, Yasunaga J, Nishikata I, Morishita K, Matsuoka M. Aberrant expression of the MEL1S gene identified in association with hypomethylation in adult T-cell leukemia cells. Blood. 2004; 103:2753–2760. [PubMed: 14656887]

Yu H, Neale G, Zhang H, Lee HM, Ma Z, Zhou S, Forget BG, Sorrentino BP. Downregulation of Prdm16 mRNA is a specific antileukemic mechanism during HOXB4-mediated HSC expansion in vivo. Blood. 2014; 124:1737–1747. [PubMed: 25082879]

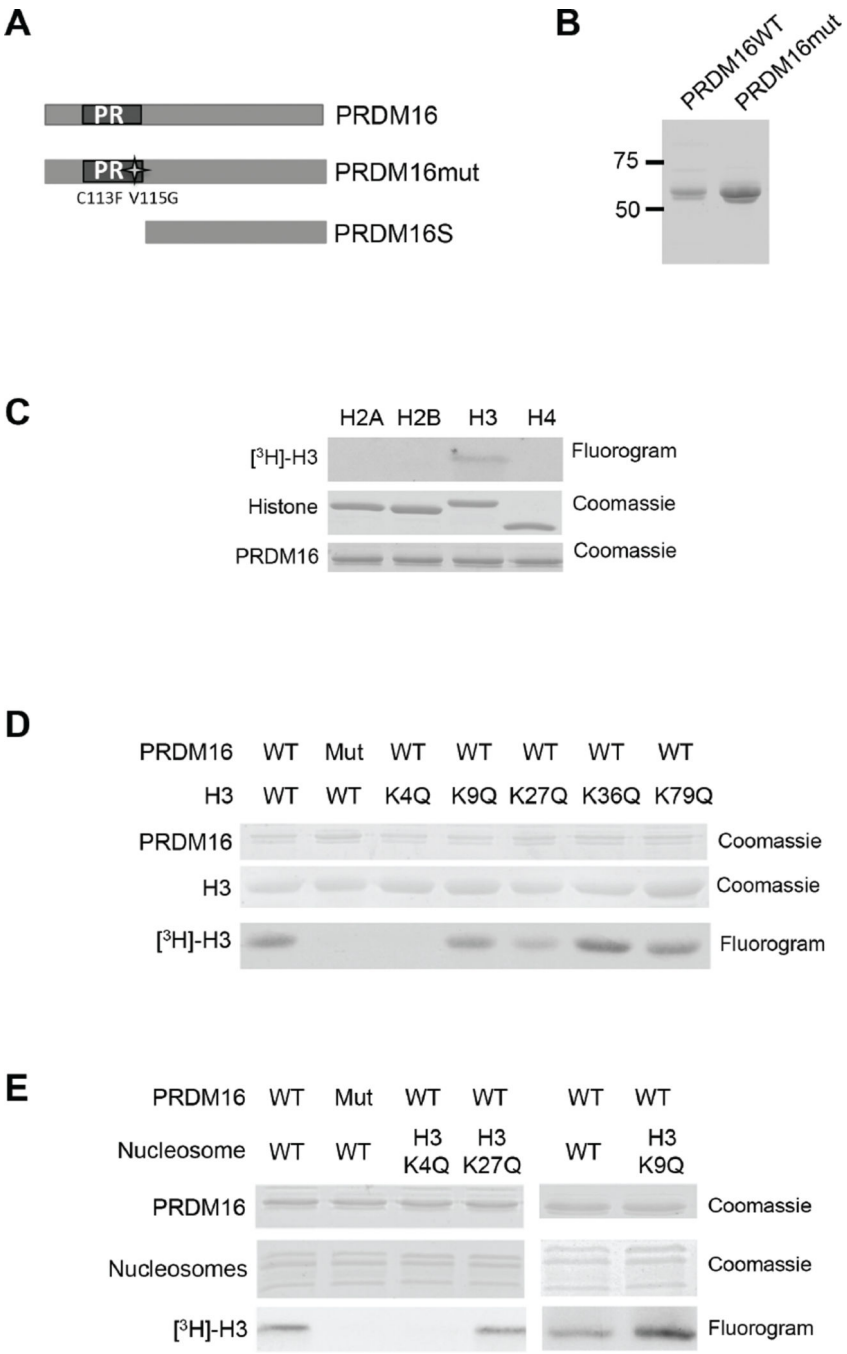

Figure 1. PRDM16 specifically methylates histone H3 K4 on nucleosomes

(See also Figure S1). **A**. Schematic representation of PRDM16, PRDM16mut and PRDM16S. The mutations in PRDM16mut are shown on bottom of the PR domain. **B**. Coomassie-stained SDS-PAGE gel of the His-tagged PR-domains of PRDM16 and PRDM16mut purified from insect cells. **C, D, E**. *In vitro* HMT assays using free recombinant histones (C), recombinant wild type histone H3 or H3 mutants with individual lysine to glutamine mutations (D), or recombinant nucleosomes (E) as the substrates. The

fluorograms for [^{3}H]-H3 methylation as well as coomassie gels for loading controls were included as indicated on right.

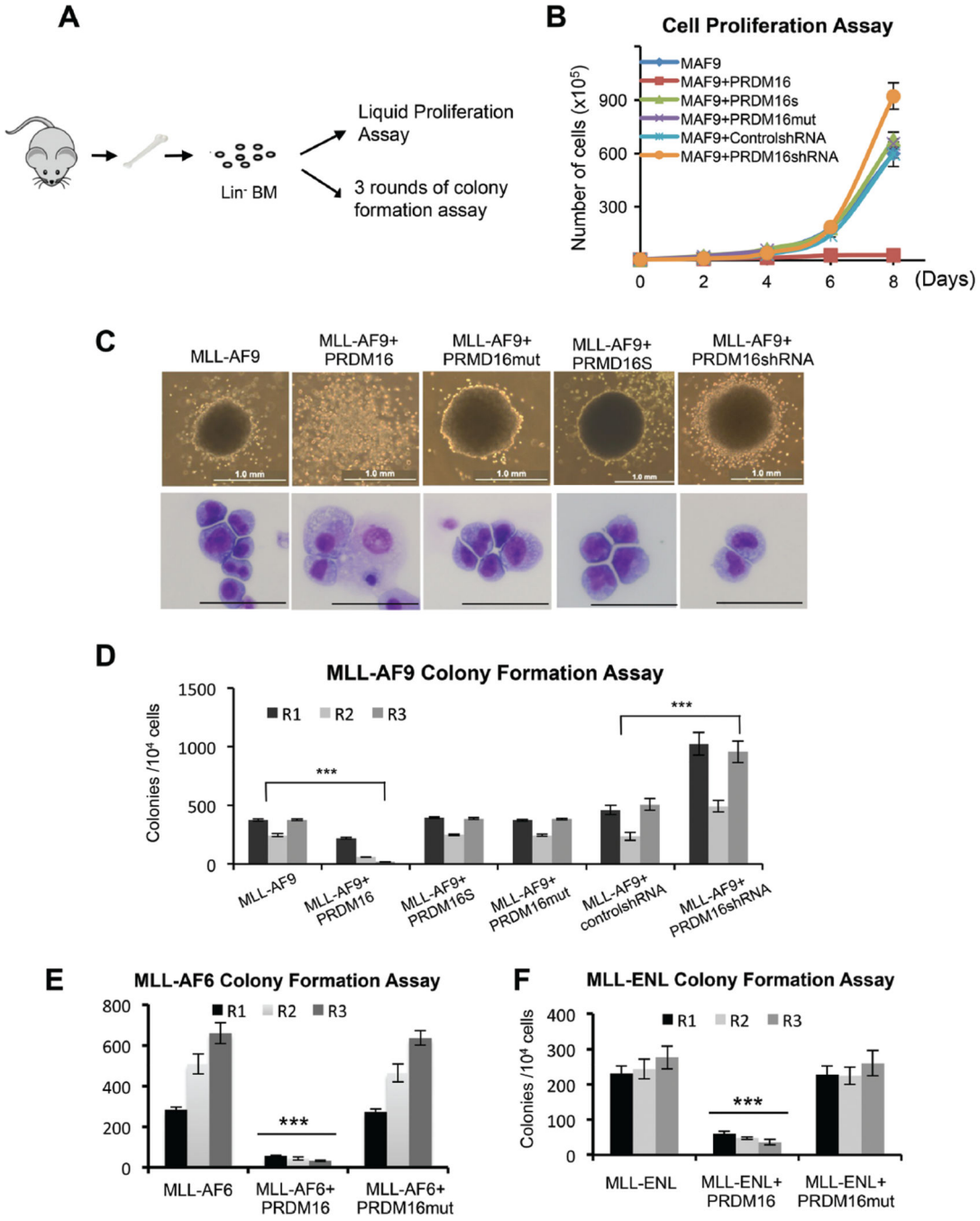

Figure 2. PRDM16 methyltransferase activity inhibits MLL-AF9 transformation *in vitro*

(See also Figure S1, S2). **A**. Schematic for the *in vitro* proliferation and colony formation experiments. **B**. Cell proliferation assay for MLL-AF9 (MAF9) with or without overexpression of PRDM16, PRDM16mut, PRDM16S as well as MLL-AF9 with or without PRDM16 shRNA mediated depletion. Error bars indicate standard deviation (SD) from duplicates. The results were repeated at least three times. **C**. Representative colonies (top) and Wright-Giemas-stained cells (bottom) from the tertiary plating were shown. Scan bar: 50μm. Genes used in co-transduction were indicated on top. **D**. Myeloid colony formation

assay for co-transduced bone marrow cells as indicated on bottom. Colony counts were summarized from primary, secondary and tertiary plating on methycellulose medium in the presence of IL3, IL6, SCF and GM-CSF. Error bars indicate SD from duplicates. The results were repeated at least three times. **(E, F)**. Myeloid colony formation assay for co-transduced bone marrow cells as indicated on bottom. Means and standard deviations (as error bars) were derived from at least three experiments. For **(D–F)**, ***, $p<0.0001$, two-way ANOVA test.

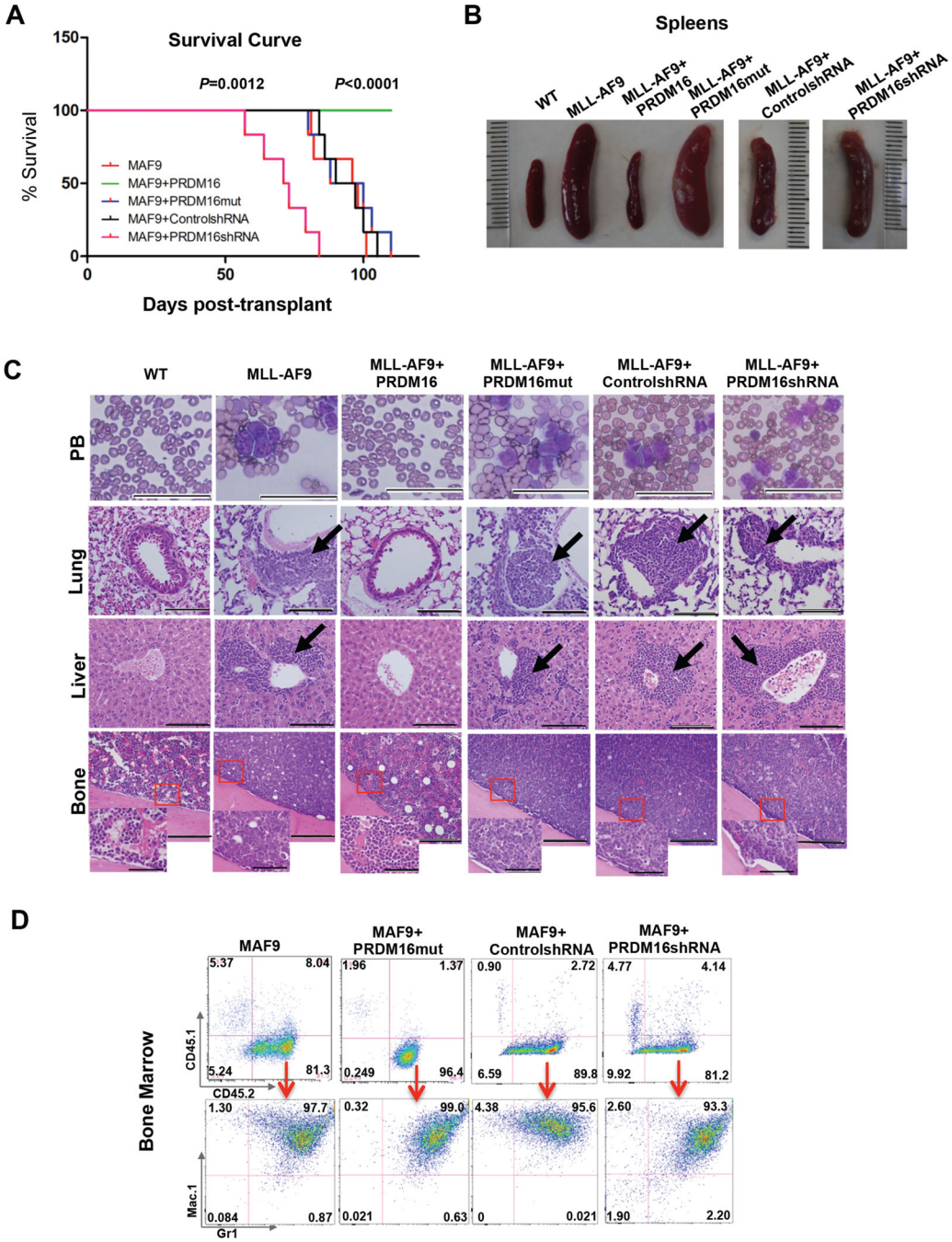

Figure 3. PRDM16 represses MLL-AF9 leukemia *in vivo*

(See also Figure S2). **A**. Kaplan-Meier survival curves for recipient mice engrafted with cells as indicated (n=6). Mantel-Cox test was performed to obtain *p* values for overexpression ($p<0.0001$) and knockdown ($p=0.0012$) experiments, respectively. **B**. The representative images of the spleens from recipient mice at the end point of the study. **C**. Representative Wright-Giemsa staining of peripheral blood (PB) smear (Scan bar: 50μm) and H&E staining of lung (Scan bar: 100μm), liver (Scan bar: 100μm) and bone (Scan bar: 200um and 50μm) as indicated on right. Co-transduced genes were indicated on top. **D**.

Representative flow cytometry analyses of bone marrow cells isolated for each group of recipient mice as indicated on top. Top row: antibodies against CD45.1 and CD45.2 surface markers to separate supporter cells and donor cells. Bottom row: antibodies against myeloid surface markers Mac-1 and Gr-1 to identify leukemic cell population. Percentage of cells for each immnophenotype was indicated in each quadrant.

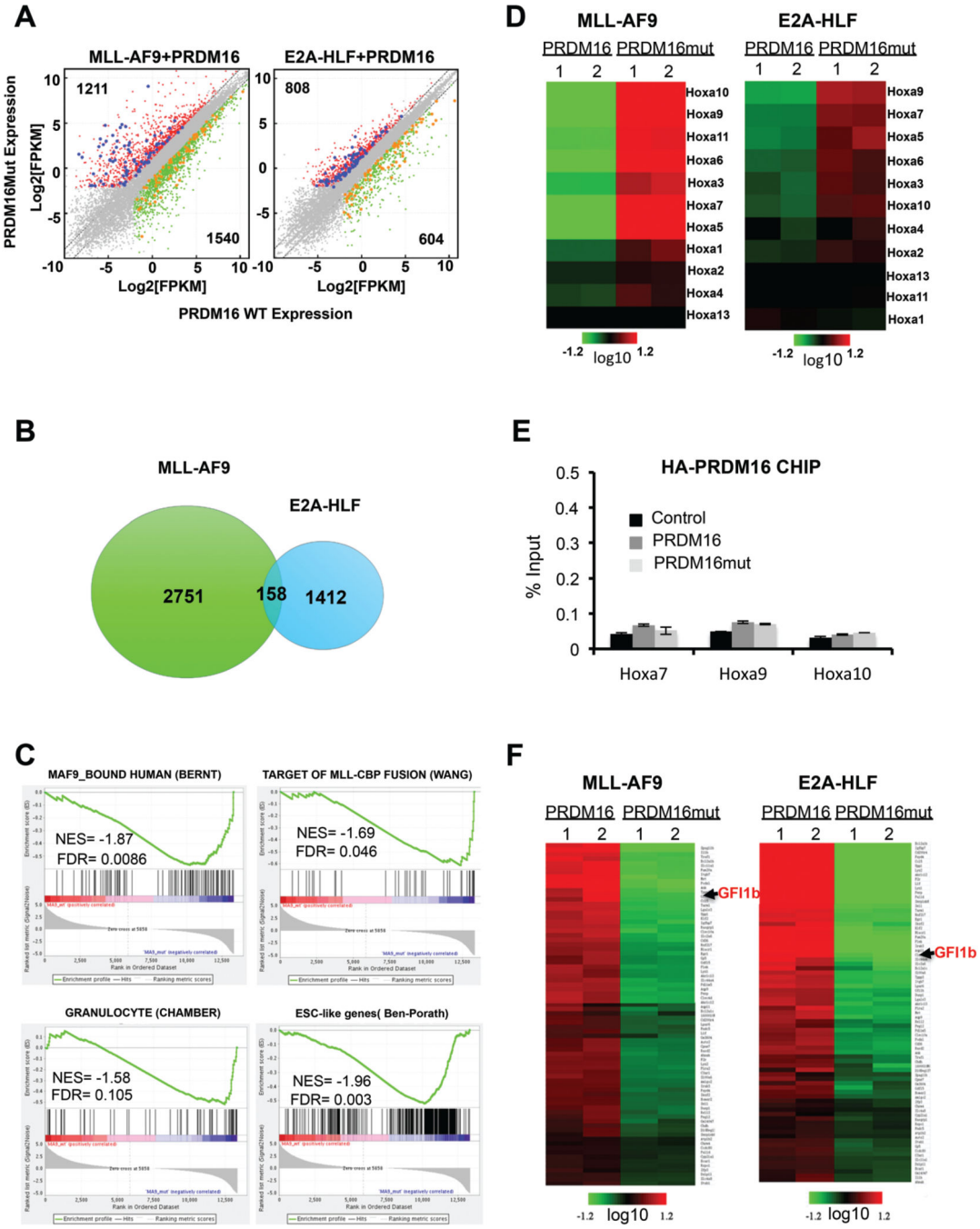

Figure 4. PRDM16 regulates broad transcriptome in MLL-AF9 and E2A-HLF cells

(See also Figure S3 and Table S1–3). **A**. Left, scatter plot for transcripts in *MLL-AF9+Prdm16mut* down regulated (X-axis) and *MLL-AF9+Prdm16mut* up regulated (Y-axis). Right, scatter plot for transcripts in *E2A-HLF+Prdm16* down regulated (X-axis) and *E2A-HLF+PRDM16mut* up regulated (Y-axis). Transcripts levels were presented as log2 FPKM (fragments per kilobase of transcript per Million mapped reads). Genes that have > 2 fold differences in expression as well as <=0.05 FDR corrected *p*-value in each cell type are represented by red and green dots for up and down regulated genes, respectively. Grey, genes

with no expression change in either cell type. Blue dots, genes expressed higher in both *MLL-AF9+Prdm16mut* and *E2A-HLF/Prdm16mut* co-transduced cells. Orange dots, genes expressed higher in both *MLL-AF9+Prdm16* and *E2A-HLF+Prdm16* co-transduced cells. **B**. Venn diagram for the differentially expressed genes upon inactivation of PRDM16 in co-transduced MLL-AF9 or E2A-HLF cells. **C**. Gene set enrichment analysis (GSEA) on genes regulated by PRDM16 methyltransferase activity in MLL-AF9 co-transduced cells. NES: normalized enrichment score. FDR: false discovery rate. References see text. **D**. Heat map for *Hox A* genes (indicated on right) in *MLL-AF9* and *E2A-HLF* cells as indicated on top. Color bar indicates scale of log2 fold change after centering of expression values. Duplicate RNA-seq data sets were used. **E**. ChIP for exogenous PRDM16 at *Hox A* genes (X-axis). Anti-HA antibody is used. Signals for each experiment were normalized to 1% input. Means and standard deviations (as error bars) from at least three independent experiments were presented. **F**. Heat map for genes that have lower expression in *PRDM16mut+MLL-AF9* and *PRDM16mut*+E2A-HLF cells as indicated on top. Color bar indicates scale of log2 fold change after centering of expression values.

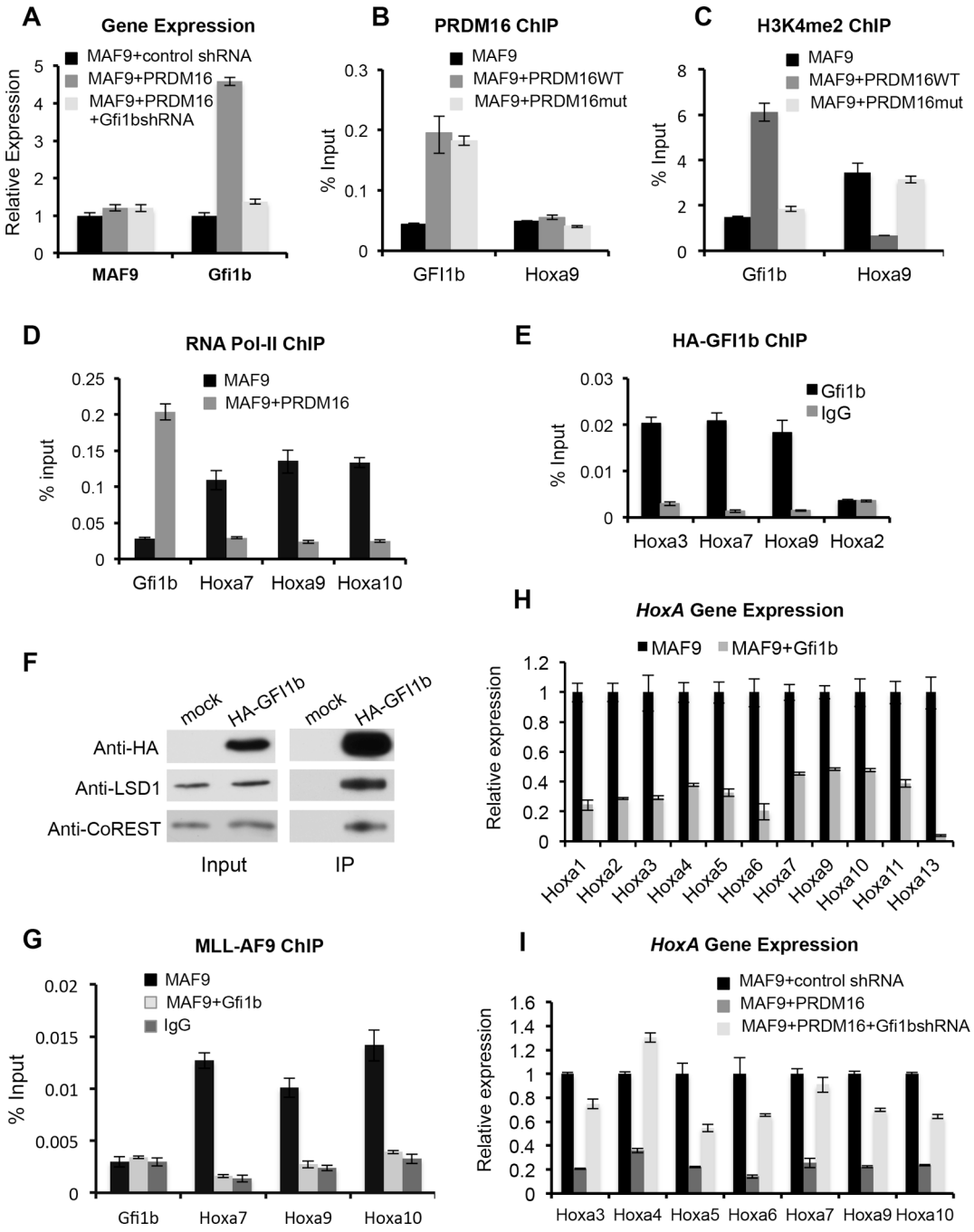

Figure 5. Gfi1b is the key intermediate in PRDM16 regulation of *Hox A* genes

(See also Figure S4, S5). **A**. Real-time PCR for *MLL-AF9* and *Gfi1b* with or without PRDM16 overexpression and Gfi1b knock-down. Gene expression was normalized against *GAPDH* and presented as fold change against the level in MLL-AF9/control shRNA cells, which is arbitrarily set at 1. **(B-E and G)**. ChIP experiments using antibodies as indicated on top. Signals for each experiment were normalized to 1% input. B, E, anti-HA antibody was used to detect exogenous PRDM16 or GFI1b. G, anti-Flag antibody was used to detect FLAG-MLL-AF9. **F)** Immunoprecipitation of exogenous HA-GFI1b using anti-HA antibody

in *MLL-AF9+Gfi1b* cells. Antibodies were indicated on left. (**H)**. Real-time PCR for *Hox A* genes in *MLL-AF9* cells with or without *Gfi1b* overexpression. (**I)**. Real-time PCR for *Hox A* genes in *MLL-AF9* or *MLL-AF9+PRDM16* cells treated with control or *Gfi1b* shRNAs as indicated. For H and I, gene expression was normalized against *GAPDH* and presented as fold change against the level in MLL-AF9, which is arbitrarily set at 1. For A–G and I, means and standard deviations (as error bars) from at least three independent experiments were presented.

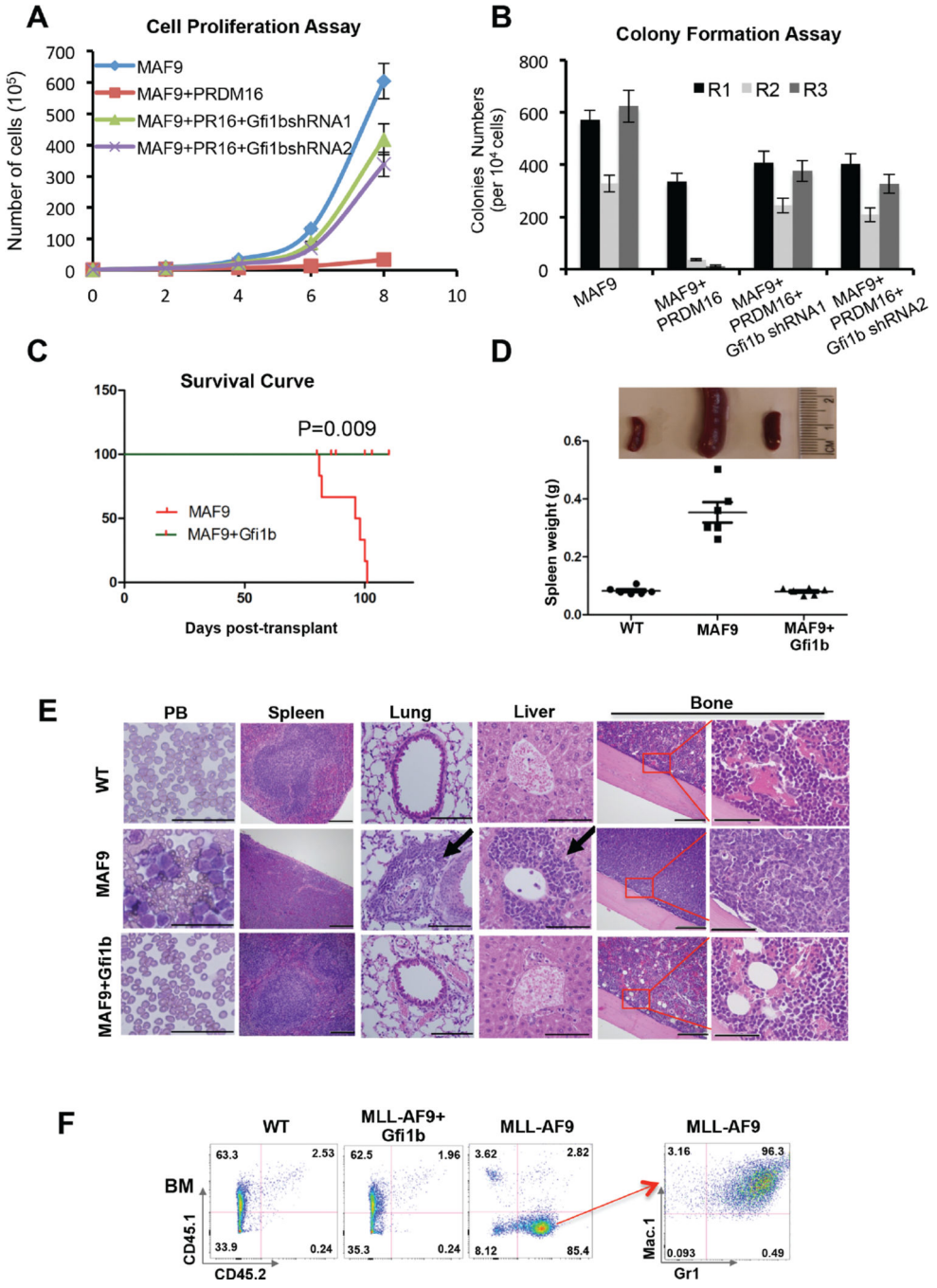

Figure 6. Gfi1b overexpression inhibits MLL-AF9 leukemogenesis

(See also Figure S6). **A**. Liquid cell proliferation assays. Cell number (Y-axis) is counted every two days (X-axis). Error bars indicate SD from duplicates. The results were repeated at least three times. **B**. Myeloid colony formation assay. Colony counts from primary (R1), secondary (R2), and tertiary (R3) plating were summarized for each co-transduction as indicated on bottom. Means and SD (error bars) from duplicates were presented. The results were repeated at least three times. **C**. Kaplan-Meier survival curve of cohorts of recipient mice (n=6). *p*-value was calculated using the Mantel-Cox test. **D**. Top, representative image

of spleens from the recipient mice. Bottom, the distribution of the spleen weight for each cohort. The MLL-AF9 cohort was the same as shown in Figure 3 since the experiments were performed at the same time. **E**. Wright-Giemsa staining of peripheral blood (PB) smear and histology of organs (H&E staining) of recipient mice (as indicated on top) at the end point of the study. Scan bars: 50μm for PB, 200μm for spleen, 100μm for lung and liver, 200μm and 50μm for bones. **F**. Representative flow cytometry analysis of BM cells in each cohort. Antibodies included CD45.1 vs. CD45.2 (left panels) and Mac-1 vs. Gr-1 (right panel) as indicated. Percentage of cell population was indicated in each quadrant.

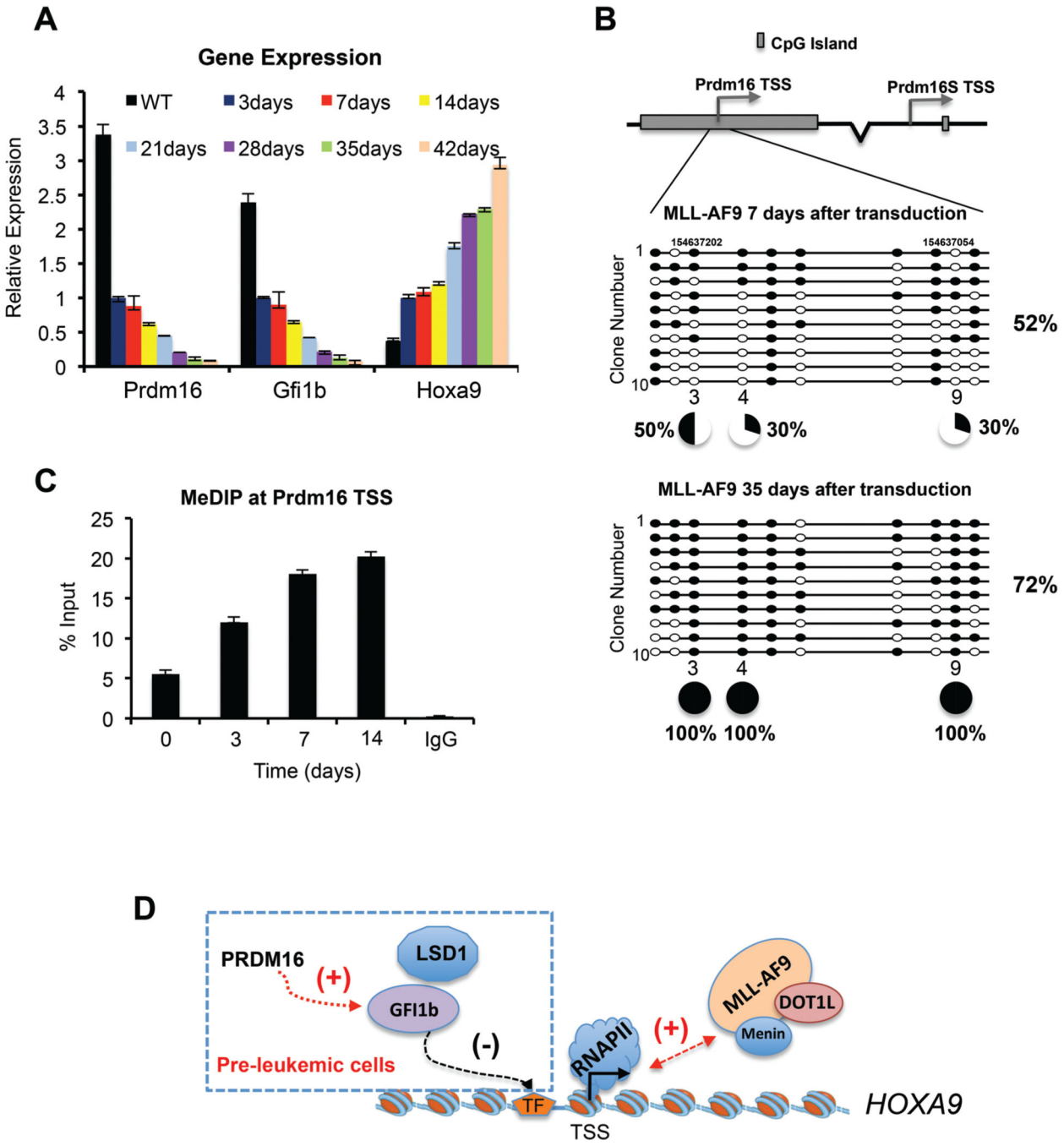

Figure 7. PRDM16 is regulated by DNA methylation

(See also Figure S7). **A**. Real-time PCR for *Prdm16, Gfi1b and Hoxa9* gene expression in pre-leukemic MLL-AF9 cells. Gene expression was normalized against *GAPDH* and presented as fold change against their respective levels in cells 3-day after transduction, which was arbitrarily set at 1. **B**. Top, schematic of CGIs at PRDM16 and PRDM16S. Bottom, bisulfite-sequencing results for 10 clones in each experimental group as indicated on top. Percentage of total methylated CpG sites was indicated on right and percentage of methylation at selected CpG sites were indicated on bottom. **C**. MeDIP was performed at

different time after MLL-AF9 transduction as indicated on bottom. DNA corresponding to TSS of PRDM16 was amplified by real-time PCR. Signals for IP were normalized to 1% input. Means and standard deviations (as error bars) from at least three independent experiments were presented. **D**. Schematic for the PRDM16 mediated regulation in pre-leukemic cells. See text for detail.